Research Article

Enhancing Mechanical Properties of PLA Filaments through Orange Peel Powder Reinforcement: Optimization of 3D Printing Parameters

Muthu Natarajan Shunmugam*, Senthil Sankaranarayanan, Narayanasamy Pandiarajan and Balasubramanian Karthekeyan Parrthipan
Department of Mechanical Engineering, Kamaraj College of Engineering and Technology, Near Virudhunagar, Madurai, Tamil Nadu, India

Balasundar Pandiarajan
Department of Mechatronics Engineering, Kamaraj College of Engineering and Technology, Near Virudhunagar, Madurai, Tamil Nadu, India

* Corresponding author. E-mail: smnrajan25@gmail.com DOI: 10.14416/j.asep.2024.08.011
Received: 15 April 2024; Revised: 20 June 2024; Accepted: 2 August 2024; Published online: 28 August 2024

Abstract
This study investigates the augmentation of the mechanical properties of Polylactic Acid (PLA) filaments by incorporating Orange Peel Powder (OPP) as an eco-friendly filler for 3D printing applications. The study delves into optimizing the printing parameters to achieve enhanced mechanical characteristics while maintaining printability. Various 3D printing process parameters were analyzed systematically to assess their impact on tensile strength, flexural strength, and impact resistance. A thorough investigation was conducted to determine the impact of layer height, infill density, and printing speed on the overall mechanical properties of the printed specimens. The findings demonstrate that adding 25% OPP significantly enhances the mechanical strength of the PLA composite without compromising printability, with optimal concentration and printing parameters identified. Thermo gravimetric study reveals that the PLA/OPP composite filament has a higher maximum thermal degradation temperature of 329 °C, compared to the PLA's temperature of 316 °C. This research contributes to advancing the development of sustainable and mechanically robust materials for additive manufacturing, offering insights into the fabrication of PLA-based biodegradable composites tailored for specific applications in various industries.

Keywords: Bio-degradable filler, Optimization, Orange peel powder, Polylactic acid, Printing parameters, 3D printing

1 Introduction

Fused Deposition Modelling (FDM) fabricates products by extruding materials through a nozzle and joining them to manufacture three-dimensional objects [1]. The additive manufacturing industry has become increasingly intrigued by polylactic acid (PLA) due to its biodegradability, renewability, and processing simplicity. Various studies have focused on improving its mechanical properties to expand its applications [2]–[4]. Moreover, the work of Saini *et al.*, investigated the influence of various techniques, such as annealing and blending, on the mechanical properties of PLA [5]. They reported that altering processing conditions can effectively modify PLA's mechanical characteristics, enhancing its suitability for diverse applications.

Numerous investigations have been conducted to improve the mechanical properties of 3D printing materials by adding reinforcements into polymer matrices [6]. Research by Parandoush *et al*., investigated the reinforcement of PLA; the incorporation of fibers enhanced the material's tensile strength and resistance to impact [7]. New filaments

with natural filler reinforcements have been extensively studied for their ability to improve the strength, stiffness, and thermal properties of polymers [8]. For instance, the review conducted by Romani *et al*., focused on incorporating biomass waste materials into PLA composites via extrusion-based additive manufacturing, where improved mechanical properties and thermal stability are achieved [9]. Similarly, the utilization of natural fillers and waste materials as reinforcements has gained attention due to their sustainability and cost-effectiveness. Studies by Lohar *et al*., explored the reinforcement of polymers using agricultural waste-derived materials, demonstrating promising results in enhancing mechanical properties while simultaneously reducing environmental impact [10].

The process parameters of 3D printing play a vital role in the performance of the 3D printed objects. This study's chosen parameters include layer height, infill density, and printing speed. Layer height refers to the thickness of each material layer deposited during the 3D printing process. It is a critical parameter that influences the resolution, surface finish, and overall quality of the printed object. Infill density refers to the amount of material used to fill the interior of a 3D-printed object, expressed as a percentage. It determines the internal structure's strength, weight, and material usage. Printing speed refers to the rate at which the print head moves while extruding material, usually measured in millimeters per second (mm/s). It affects the overall print time and the quality of the printed object.

Optimizing 3D printing parameters is crucial for superior mechanical properties and part quality. Numerous studies have investigated the influence of printing parameters, including layer height, infill density, printing speed, and temperature, on the mechanical performance of printed parts [11]. For example, the work by Croccolo *et al*., investigated the effect of varying printing temperatures on the tensile strength and layer adhesion of 3D-printed PLA parts, highlighting the importance of temperature control in achieving optimal mechanical properties [12]. The performance of 3D printing products depends on various parameters such as layer height, infill density, printing speed, build orientation, raster angle, infill pattern, extrusion temperature, and bed Temperature as reported in the previous works [13]–[15].

The effects of using natural fibers, such as silane fibers, Nona/Soy fillers, palm fiber, *Ceiba petandra* fiber, timoho fiber and several agro waste natural fillers to enhance the mechanical properties, printability, and performance of the resulting composite filaments were explored earlier which gives an idea about the fabrication and testing of the composite filament [16]–[22]. This study provides a foundational understanding of the existing research related to PLA enhancement, reinforcement materials, and optimization of 3D printing parameters, setting the stage for the manuscript's focus on enhancing PLA filament properties by incorporating orange peel powder and optimizing printing conditions.

2 Materials and Methods

2.1 *Materials*

The study utilized several raw materials, including polylactic acid (PLA), orange peel powder, and wax. The PLA was sourced from Sigma Aldrich Chemicals Private Limited in Bengaluru. The orange peel extract was obtained from MM Stores, Madurai district, Tamil Nadu, India. The extract was initially cleaned and soaked in distilled water to prepare the orange peel for 24 h. This soaking effectively removed impurities and foreign particles from the orange peel extract. The extract was then sun-dried for three days to reduce its moisture level. Subsequently, it was heated to 80 °C in a vacuum air oven for five hours. After the orange peel extract had dried, it was pulverized at 350 rpm with a mechanical pulverizer for sixty minutes. A cooling process was implemented in the pulverization chamber at 5-min intervals. This created the pulverized orange peel filler, as shown in Figure 1. The micrograph of orange peel powder is given in Figure 2.

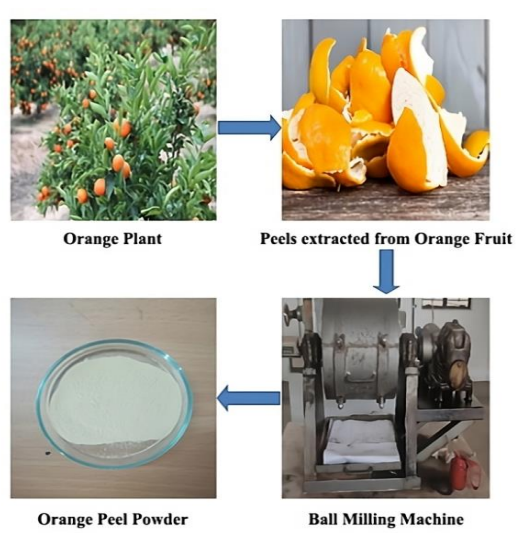

Figure 1: Orange peel powder preparation process.

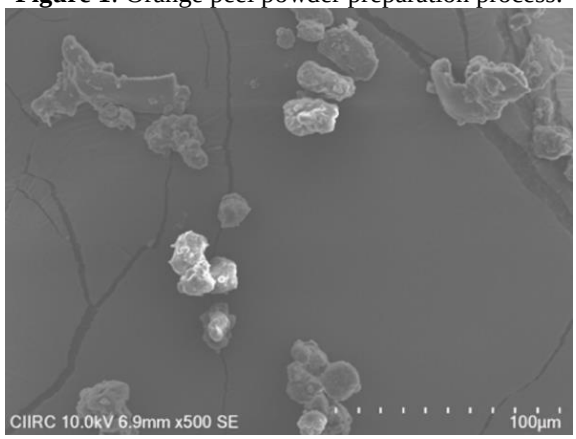

Figure 2: Micrograph of OPP.

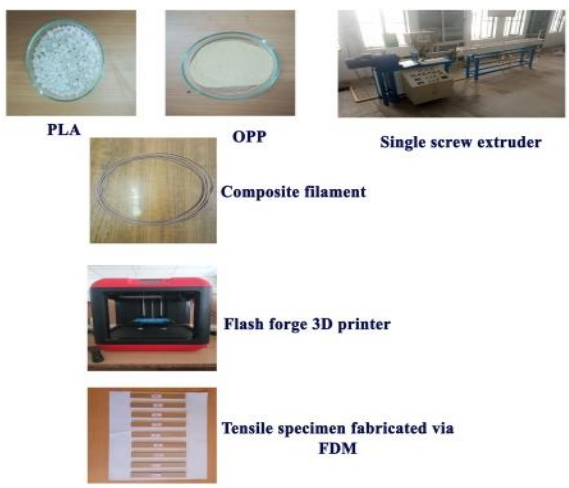

Figure 3: Fabrication of composite filament.

2.2 *Composite filament fabrication*

Before the compounding process, the PLA granules and orange peel powder were dried at 80 °C for 5 h in an oven with air circulation. Subsequently, they were combined in their dry state. The dry mixture consisted of PLA granules (75 wt.%) and orange peel powder (25 wt.), and this mixture was fed into a single screw extruder equipped with a blending feed hopper. The extrusion process was carried out at a constant speed of 20 mm/s. The temperature along the entire extrusion path, from the feeding zone to the die, was maintained at an average of 160 °C. The extruded filament, with a diameter of 1.75 mm (Figure 3), was rapidly cooled in a water tank with a temperature range of 20–30 °C. Subsequently, it was wound onto a spool using a winding mechanism. The diameter of the filament prepared is 1.75 mm.

2.3 *Particle size analysis*

The size of particles significantly impacts the efficiency of manufacturing processes and the overall quality of the final product. The Malvern Particle Size Analyzer Instrument was employed to thoroughly analyze the filler's particle dimensions to assess the particle size. This analysis yielded results in cumulative wt.% distribution and particle size distribution frequency percentage.

2.4 *Fourier Transform Infrared Spectroscopy (FTIR)*

The process of determining the chemical functional groups that are inherent in the filaments derived from PLA/orange peel powder was accomplished through FTIR analysis. FTIR data was collected at room temperature using an RXI Perkin Elmer FTIR spectrometer, covering the range from 4000 to 500 cm^{-1}, with a resolution of 4 cm^{-1}.

2.5 *X-ray diffraction test (XRD)*

X-ray diffraction analysis was performed on filament made from PLA and orange peel powder utilizing a Bruker D8 X-ray Diffractometer. The generator settings were 40 kV and 30 mA, and the X-ray source utilized Ni-filtered Cu K radiation. The XRD pattern was obtained in reflection mode with a scan rate of 50/min, covering the range from 0° to 80°.

The filaments' Crystallinity Index (CI) was calculated using the standard peak height technique as indicated in Equation (1).

$$I_C\ (\%) = \left(1 - \frac{I_{am}}{I_{cp}}\right) \times 100 \quad (1)$$

I_{cp} is the intensity of the crystalline peak, and I_{am} - is the intensity of the amorphous peak.

2.6 *Thermo Gravimetric Analysis (TGA)*

Thermogravimetric analyses of the matrix (PLA) and the fillers (AC and OPP) were conducted using a Thermogravimetric Analyzer (TA Instrument: NETZSCH STA 449F3 STA 449F3A – 1100 –M). To assess the thermal stability of the samples, they were subjected to a gradual heating process at a rate of 10 °C/min within the temperature range of 300 °C to

550 °C, all while maintaining a dynamic flow of nitrogen (50 mL/min). Each test involved approximately 10.2 mg of the samples placed on an alumina crucible, and during this process, weight loss occurred with every 100 °C increase in temperature.

2.7 *Soil burial test*

In accordance with ASTM D5988 guidelines, the Soil burial test was carried out. Filaments produced from PLA/AC and PLA/OPP were 3D printed with dimensions of 40 × 10 × 0.5 mm³ using a FlashForge Finder 3D printer. Subsequently, these samples were subjected to a 24-h drying process in an oven at 50 °C and then measured. To create aerobic conditions conducive to decomposition, the container containing the soil and samples was exposed to an environment with 25 °C temperature and a relative humidity of 40%–45%. Protective plastic covers were employed to shield the pots and prevent moisture loss from the soil. Daily, a digital soil analysis meter was employed to monitor the soil's relative humidity. The biodegradation rate was assessed by tracking changes in weight over time since the burial. At intervals of 5 days, the soil samples were extracted, and after removing any remaining soil with distilled water, they were subjected to a 24-h conditioning period in a 50 °C oven.

2.8 *Tensile properties*

A tensile test is an essential mechanical evaluation wherein a meticulously designed specimen is loaded under controlled conditions, with the force applied and the specimen's extension over a designated distance being measured. Tensile properties are typically determined through this test, often following an ASTM standard procedure. The tensile testing was performed using a Deepak Poly Plastic Universal Testing Machine with specimens measuring 100×20×8 mm³, printed on a flat surface by ASTM Standard D 3039 [23]. The specimens were prepared using a Flash Forge finder 3D printer (Nozzle diameter of 0.4 mm, extrusion temperature of 210 °C, bed temperature of 45 °C).

2.9 *Flexural properties*

The flexural test assesses the force required to bend a beam under a three-point loading arrangement. This data is often employed to select materials for components that need to withstand loads without bending. The flexural modulus of a material reflects its stiffness when subjected to flexural stress. The flexural test followed ASTM Standard D 7264 using a Deepak Poly Plastic Universal Testing Machine with a three-point loading setup, using specimens measuring 220 × 20 × 10 mm³.

2.10 *Impact properties*

The impact test determines the amount of energy a material can absorb during fracture. The energy absorbed measures the material's durability and is a crucial tool for studying temperature-related shifts between brittleness and ductility. The primary objective is determining whether the material demonstrates brittle or ductile behavior. The Charpy impact test was performed using a Deepak Poly Plastic digital pendulum impact tester, following the ASTM Standard D 256 guidelines.

2.11 *Specimen preparation*

The specimens for conducting tensile, flexural, and impact tests were generated utilizing a FlashForge Finder 3D printer. These were printed by adjusting the printing parameters outlined in Tables 1 and 2, with a nozzle diameter of 0.4 mm, an extrusion temperature of 210 °C, and a bed temperature of 45 °C [24].

Table 1: Levels of input parameters.

Particulars	Level I	Level II	Level III
Layer height (mm)	0.08	0.16	0.24
Infill density (%)	60	80	100
Printing speed (mm/s)	50	70	90

Table 2: Specimen details.

Sample No.	Layer Height (mm)	Infill Percentage (%)	Print Speed (mm/s)
1	0.08	60	50
2	0.08	80	70
3	0.08	100	90
4	0.16	60	70
5	0.16	80	90
6	0.16	100	50
7	0.24	60	90
8	0.24	80	50
9	0.24	100	70

3 Results and Discussions

The main objective of this study is to disclose the outcomes of experiments carried out on 3D printing filaments made from PLA and orange peel powder. In line with prior research cited in the literature review, the concentration of fillers in the PLA matrix has been

fixed at 25wt%. This section explains the effects of natural filler concentration on various properties of the PLA matrix, including physicochemical, mechanical, thermal, fracture morphology, and soil biodegradation characteristics. The experimental findings are presented through micrographs, charts, images, and tables, categorizing each PLA-based 3D printing filament type.

3.1 *Particle size analysis of fillers*

A particle size analyzer was employed to assess the particle dimensions of the natural fillers [25]. It is important to note that the particle size of these fillers within the polymer matrix exerts a substantial influence on the filaments' mechanical, physical, and thermal characteristics, as emphasized in the work by Ghabezi *et al*., [26]. Figure 3 illustrates the particle size characteristics of orange peel powder (OPP). This data emphasizes that the OPP exhibits a particle size below 20 µm, with an average particle size of 9 µm, as depicted in Figure 4. This is visually depicted in Figure 4, underscoring the finely refined nature of the orange peel powder. This dimensionality information regarding the OPP is pivotal, demonstrating its fine particle size distribution and emphasizing its potential impact on the overall properties of the composite material.

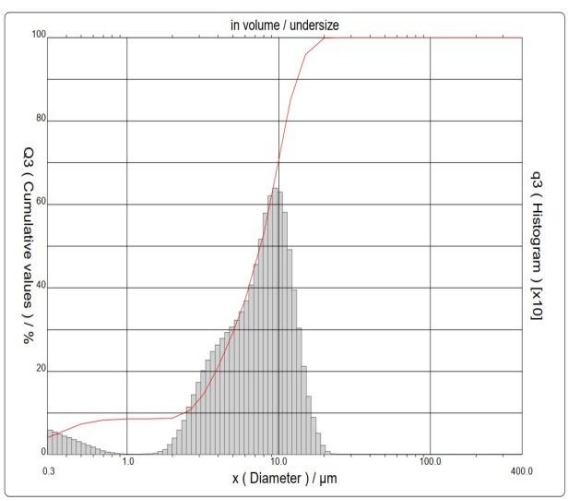

Figure 4: Average particle size of OPP fillers.

3.2 *Chemical composition analysis of OPP filler*

The process established by Kurshner and Hoffer was followed to calculate the quantity of cellulose in the OPP. The hemicellulose content in the OPP was calculated based on the protocol suggested in the NFT 12-008 standard. The step-by-step guidelines in the APPITA P11s-78 standard were followed to finalize the lignin content in OPP. The thermal decomposition characteristics, mechanical properties, and overall durability of composite materials are entirely determined by the chemical composition of the infill material. The source of the plant significantly influences the chemical composition of plant-based fillers. In the case of OPP, its composition includes approximately 69.23 wt% cellulose, 19.28 wt% lignin, 9.23 wt% hemicellulose, and a minor content of 0.19 wt% wax. Furthermore, the filler contains approximately 0.0502 wt% ash.

3.3 *FTIR analysis*

The FTIR spectra of the PLA matrix and the OPP filler exhibited broader peaks when measured at equivalent wavelengths. These peaks observed at 3669 cm^{-1} and 3560 cm^{-1} are attributed to the hydroxyl (-OH) group in the OPP filler and the PLA group, respectively. The overlapping peaks at 1618 cm^{-1} and 1748 cm^{-1} indicate that the carboxyl (C=O) group of hemicellulose plays a role in preventing the autolysis of the acetyl group. In the case of PLA, additional groups were observed at 1544 cm^{-1}, corresponding to the (-CO of carbonate) [27]. These hydroxyl and carbonyl groups contribute to the compatibility between the matrix and reinforcement and facilitate hydrogen bonding. As illustrated in Figure 5, it is noteworthy that the filament manufacturing process does not produce any new chemical by-products. The PLA/OPP filament spectra appeared to flatten, probably due to interactions between the polar groups on the OPP infill and the hydroxyl group of PLA.

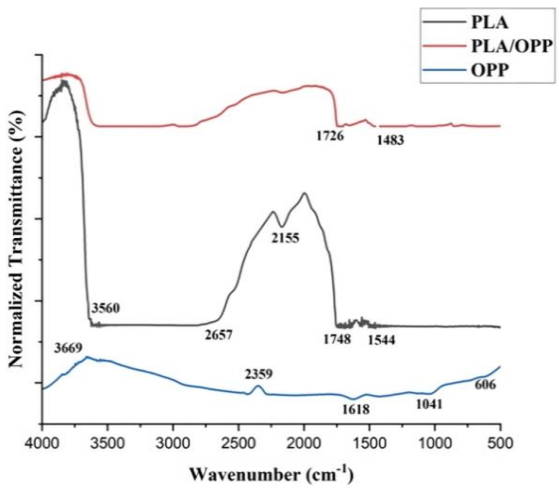

Figure 5: FTIR spectra for PLA, OPP, and PLA/OPP.

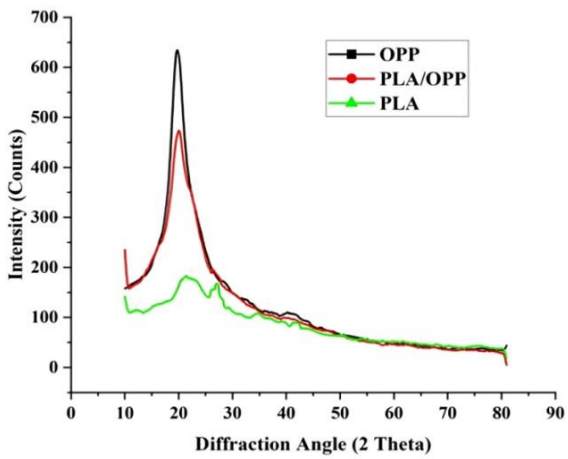

Figure 6: X-Ray diffractograms of PLA, OPP, and PLA/OPP.

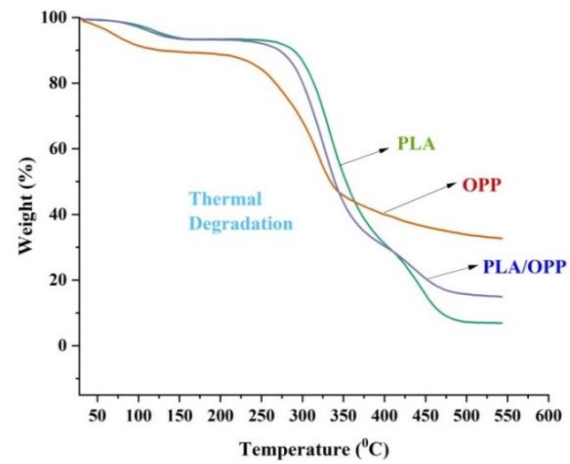

(a)

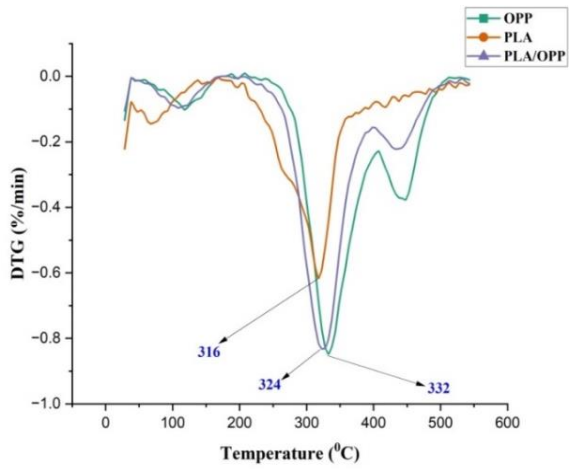

(b)

Figure 7: TGA results of PLA, OPP, PLA/OPP filament (a) Primary thermogram and (b) Derivative thermograms.

3.4 *X-ray diffraction analysis*

X-ray diffraction is a technique utilized to determine the compatibility and dispersion of a natural substance and polymer matrix and to analyze the presence of amorphous and crystalline phases in films [28]. Figure 6 shows the X-ray diffraction patterns of OPP, PLA, and their composite. The crystallinity index of the OPP was determined to be 69.85%. A higher crystallinity index is associated with enhanced tensile strength in filaments. In contrast, PLA displays a prominent peak at $2\theta = 19.60°$, indicating lower crystallinity.

Conversely, the composite filament exhibits a more distinct peak at $2\theta = 23.65°$ compared to the PLA filament, signifying a higher degree of crystallinity in the PLA/OPP filament. The PLA/OPP composite displays a crystallinity index of 66.11%, surpassing the pure PLA value of 47.23%. This clear indication of high crystallinity in the filaments significantly impacts their thermal stability and mechanical strength.

3.5 *Thermogravimetric analysis*

To investigate the thermal stability of PLA, orange peel filler, and PLA/OPP, thermal gravimetric analysis (TGA) was conducted. Figure 7 present the TGA and DTG curves for PLA, OPP, and PLA/OPP. The primary thermograms (TGA) of the PLA/OPP filament reveal the weight loss of the films with increasing temperature, while the derivative thermograms (DTG) provide information about the degradation temperature at each stage. Due to its

lignocellulosic nature, the orange peel filler exhibited a gradual degradation process and withstood higher temperatures than the PLA matrix [29]. Notably, the maximum degradation temperatures for the PLA and PLA/OPP filaments were determined to be 316 °C and 329 °C, respectively.

Figure 7 illustrates that the increased thermal stability of the orange peel filler elevated the maximum degradation temperatures of PLA from 316°C to 329 °C in the case of PLA/OPP filaments. The observed enhancement may be related to the chemical interaction and interfacial bonding between PLA and OPP. Since OPP possesses greater thermal stability than PLA, its reinforcement with PLA has enhanced the filaments' thermal stability.

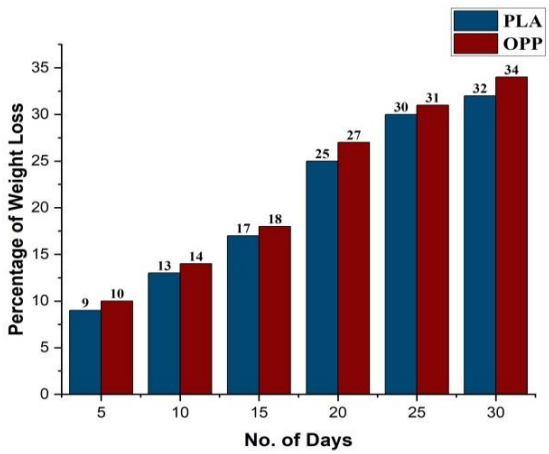

Figure 8: Weight loss (%) due to soil degradation for PLA/OPP.

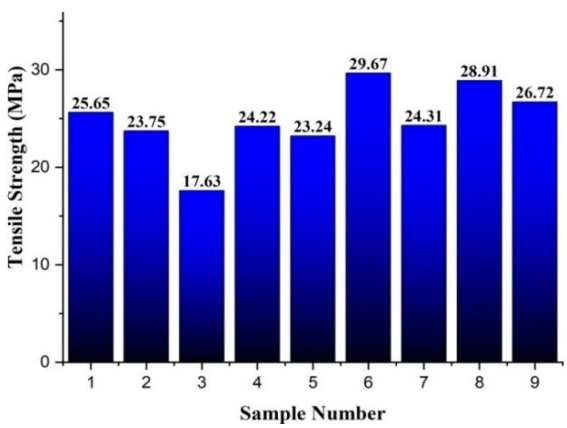

(a)

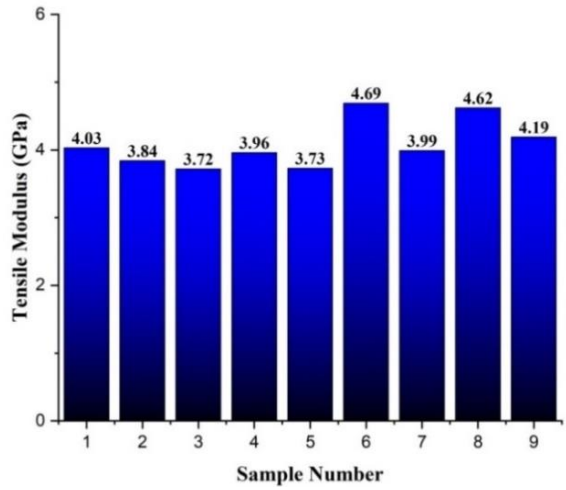

(b)

Figure 9: Tensile properties of PLA/OPP as (a) indicates the tensile strength and (b) indicates the tensile modulus of the composite filaments.

3.6 *Soil biodegradation test*

Figure 8 illustrates how the weight loss of controlled PLA and PLA/OPP composites containing 25% OPP evolved as they underwent degradation in the soil. Within 30 days, the presence of OPP in the composite accelerated the rate at which the PLA/OPP specimen decomposed in the soil. This heightened decomposition rate in the presence of the natural filler OPP can be attributed to enzyme oxidation, effectively expediting the degradation of the PLA/OPP filament. Notably, approximately 34% of the weight of the PLA/OPP specimen was lost during this process. It is crucial to incorporate the natural infill component, OPP, into the PLA matrix to facilitate composites' organic decomposition. The matrix and the OPP filler exhibit water resistance, with the OPP filler being more crystalline than the PLA counterpart. This increased crystallinity, along with the formation of hydroxyl groups and hydrogen bonds between PLA and OPP, facilitates the penetration of soil vapor particles into the filament, expediting its degradation. After 30 days, the PLA/OPP composite in the soil had lost 34% of its initial weight, providing clear evidence of its biodegradability.

3.7 *Tensile properties*

The tensile testing of PLA/OPP was conducted using a tensile testing machine, and the outcomes are depicted in Figure 9. The tensile strength of the composite filament exhibits gradual variations based

on printing parameters such as layer height, infill density, and printing speed. The maximum tensile strength achieved by PLA/OPP amounts to 29.67 MPa. This remarkable tensile performance is attributed to the effective bonding between OPP and PLA molecules and the efficient transfer of stress between the PLA matrix and the filler material [30]. The figures illustrate that the sample printed with a layer thickness of 0.16 mm, an infill density of 100%, and a printing speed of 50 mm/s demonstrates the highest tensile strength, primarily due to its superior mechanical properties. Similarly, the maximum tensile modulus, which reached 4.69 GPa, was observed in this same sample, whereas the minimum tensile modulus of 3.72 GPa was recorded for a sample with a layer thickness of 0.08 mm, 100% infill density, and a printing speed of 90 mm/s. This variation could be attributed to reduced adhesion between layers when printing at higher speeds.

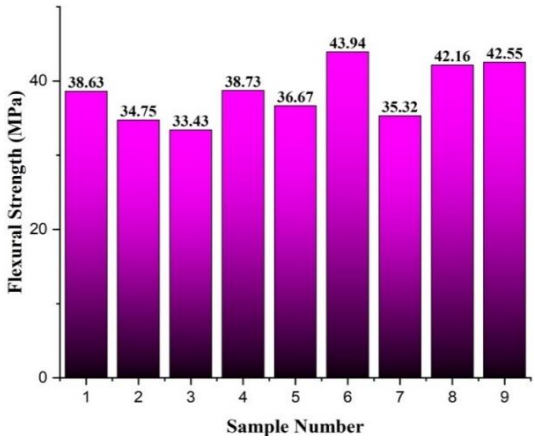

(a)

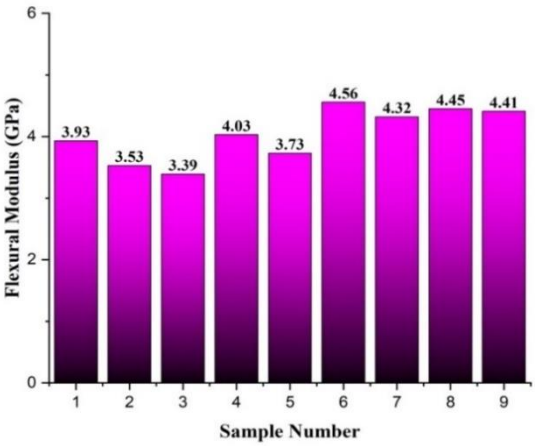

(b)

Figure 10: Flexural properties of PLA/OPP as (a) indicates the flexural strength and (b) indicates the flexural modulus of the composite filaments.

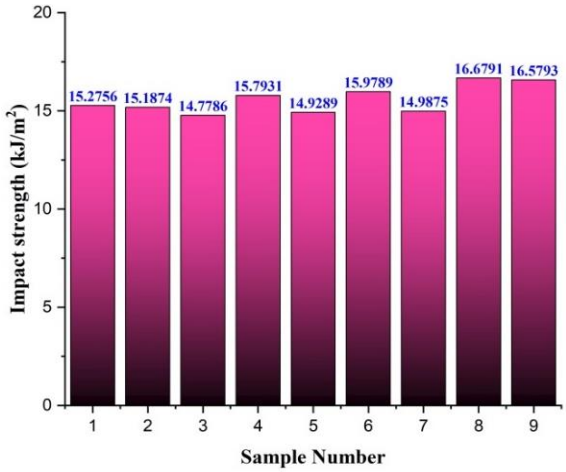

Figure 11: Impact strength of PLA/OPP.

3.8 *Flexural properties*

Flexural strength is crucial in determining the composite's ability to withstand bending loads. The flexural test results for PLA/OPP are depicted in Figure 10. It is crucial to acknowledge that the outcomes in the figures were obtained using the same printing settings as those established for the tensile testing. Similar variations can be observed in the composite material's flexural strength and tensile strength. The highest flexural strength observed in the PLA/OPP composite specimen reached 43.94 MPa. Notably, the sample printed with the same settings as the one achieving the highest tensile modulus displayed a maximum flexural modulus of 4.56 GPa. In contrast, the sample printed with a layer thickness of 0.08 mm, a 100% infill density, and a printing speed of 90 mm/s demonstrated a minimum flexural modulus of 3.39 GPa.

3.9 *Impact properties*

Impact strength reflects the ability of the composite filament to withstand sudden loads and determine how it breaks under such conditions. Figure 11, illustrates the impact strength of the PLA/OPP composite filament. The results presented in the figure were obtained using the same printing parameters as those applied in the tensile test. Notably, the sample printed with the identical settings as the one attaining the

highest tensile strength exhibited a maximum impact strength of 16.679 kJ/m^2. In comparison, the lowest recorded impact strength was 14.7786 kJ/m^2.

4 Conclusions

A composite filament was produced by employing a single screw extruder, utilizing PLA and OPP. FTIR analysis shows that both PLA and OPP exhibit hydrophilic characteristics, primarily attributed to the shared presence of the -OH band in common peaks. The utilization of OPP in the PLA matrix has led to a gradual reduction in the intensity of this peak. Notably, in the PLA/OPP filament, the presence of high-intensity peaks is not distinctly observed, indicating a high level of compatibility between PLA and OPP. XRD analyses determined that the Crystallinity Index (CI) of the PLA/OPP filament, with a 25wt% content of OPP, reached 66.11%. The XRD examination also unveiled that the PLA/OPP filament exhibits a semi-crystalline structure, which can be attributed to the coexistence of amorphous PLA and crystalline orange peel filler within the material.

Incorporating the OPP filler into PLA enhanced the filament's thermal stability, and specifically, the PLA/OPP filament with a 25% OPP content demonstrated the highest stability at elevated temperatures, notably at 324 °C. The soil biodegradation test revealed a reduction of 34% in the material's weight within 30 days. This significantly accelerates the rate of PLA degradation under identical environmental conditions. The highest recorded tensile strength and tensile modulus were 29.67 MPa and 4.69 GPa, respectively. Likewise, the sample featuring a layer thickness of 0.16 mm, a 100% infill density, and a printing speed of 50 mm/s exhibited the maximum flexural strength and modulus, determined to be 43.94 MPa and 4.56 GPa, respectively. In the future, there is the possibility to Investigate the effect of materials with shape memory properties (such as thylene-vinyl acetate, polytetrafluoroethylene, etc.) on incorporation with PLA and utilize the materials for 4D printing.

Author Contributions

All authors contributed to the study's conception and design. S.M.N.: Conceptualization, Investigation, Methodology, Formal Analysis, Writing—original draft. S.S.: Conceptualization, Supervision, Funding acquisition, Project administration, and Writing—review & editing. N.P.: Investigation, Formal analysis, Resources, Supervision, Writing - review & editing. P.K.: Investigation, Formal analysis, Resources, Visualization. B.P.: Investigation, Formal analysis, Resources, Visualization.

Conflicts of Interest

The authors declare no conflict of interest.

References

[1] A. Sola and A. Trinchi, *Fused Deposition Modeling of Composite Materials*. Sawston, UK: Woodhead Publishing, 2023.

[2] G. Rajeshkumar, S. Arvindh Seshadri, G. L. Devnani, M. R. Sanjay, S. Siengchin, J. P. Maran, N. A. Al-Dhabi, P. Karuppiah, V. A. Mariadhas, N. Sivarajasekar, and A. R. Anuf, "Environment friendly, renewable and sustainable poly lactic acid (PLA) based natural fiber reinforced composites – A comprehensive review," *Journal of Cleaner Production*, vol. 310, 2021, Art. no. 127483, doi: 10.1016/j.jclepro.2021.127483.

[3] T. M. Joseph, A. Kallingal, A. M. Suresh, D. K. Mahapatra, M. S. Hasanin, J. Haponiuk, and S. Thomas, "3D printing of polylactic acid: Recent advances and opportunities," *The International Journal of Advanced Manufacturing Technology*, vol. 125, pp. 1015–1035, 2023.

[4] L. Sandanamsamy, W. S. W. Harun, I. Ishak, F. R. M. Romlay, K. Kadirgama, D. Ramasamy, S. R. A. Idris, and F. Tsumori, "A comprehensive review on fused deposition modelling of polylactic acid," *Progress in Additive Manufacturing*, vol. 8, pp. 775–799, 2023.

[5] P. Saini, M. Arora, and M. N. V. R. Kumar, "Poly(lactic acid) blends in biomedical applications," *Advanced Drug Delivery Reviews*, vol. 107, pp. 47–59, 2016.

[6] X. Wang, M. Jiang, Z. Zhou, J. Gou, and D. Hui, "3D printing of polymer matrix composites: A review and prospective," *Composites Part B: Engineering*, vol. 110, pp. 442–458, 2017.

[7] P. Parandoush and D. Lin, "A review on additive manufacturing of polymer-fiber composites," *Composite Structures*, vol. 182, pp. 36–53, 2017.

[8] M. Calì, G. Pascoletti, M. Gaeta, G. Milazzo, and R. Ambu, "New filaments with natural fillers for FDM 3D printing and their applications in biomedical field," *Procedia Manufacturing*, vol. 51, pp. 698–703, 2020.

[9] A. Romani, R. Suriano, and M. Levi, "Biomass

waste materials through extrusion-based additive manufacturing: A systematic literature review," *Journal of Cleaner Production*, vol. 386, 2023, Art. no. 135779.

[10] D. V. Lohar, A. M. Nikalje, and P. G. Damle, "Synthesis and characterization of PLA hybrid composites using bio waste fillers," *Materials Today Proceedings*, vol. 72, no. 4, pp. 2155–2162, 2023.

[11] S. Khan, K. Joshi, and S. Deshmukh, "A comprehensive review on effect of printing parameters on mechanical properties of FDM printed parts," *Materials Today Proceedings*, vol. 50, no. 5, pp. 2119–2127, 2022.

[12] D. Croccolo, M. D. Agostinis, S. Fini, M. Mele, G. Olmi, and G. Campana, "Effects of infill temperature on the tensile properties and warping of 3D-printed polylactic acid," *Progress in Additive Manufacturing*, vol. 9, pp. 919–934, 2024.

[13] O. A. Mohamed, S. H. Masood, and J. L. Bhowmik, "Experimental Investigation and optimisation of FDM process parameters for build cost and mechanical properties using I-optimal design," *Encyclopedia of Smart Materials*, vol. 1, pp. 368–385, 2022.

[14] S. M. Natarajan, S. Senthil, and P. Narayanasamy, "Investigation of mechanical properties of FDM-processed acacia concinna–filled polylactic acid filament," *International Journal of Polymer Science*, vol. 1, pp. 1–8, 2022.

[15] N. Lokesh, B. A. Praveena, J. S. Reddy, V. K. Vasu, and S. Vijaykumar, "Evaluation on effect of printing process parameter through Taguchi approach on mechanical properties of 3D printed PLA specimens using FDM at constant printing temperature," *Materials Today Proceedings*, vol. 52, pp. 1288–1293, 2022.

[16] V. Raghunathan, V. Ayyappan, S. M. Rangappa and S. Siengchin, "Development of fiber-reinforced polylactic acid filaments using untreated/silane-treated trichosanthes cucumerina fibers for additive manufacturing," *Journal of Elastomers & Plastics*, vol. 56, no. 3, pp. 277–292, 2024.

[17] A. Vinod, J. Tengsuthiwat, R. Vijay, M. R. Sanjay and S. Siengchin, "Advancing additive manufacturing: 3D-printing of hybrid natural fiber sandwich (Nona/Soy-PLA) composites through filament extrusion and its effect on thermomechanical properties," *Polymer Composites*, vol. 45, no. 9, pp. 7767–778, 2024.

[18] A. Andoko, F. Gapsari, I. Wijatmiko, K. Diharjo, S. M. Rangappa, and S. Siengchin, "Performance of carbon fiber (CF)/*Ceiba petandra* fiber (CPF) reinforced hybrid polymer composites for lightweight high-performance applications," *Journal of Materials Research and Technology*, vol. 27, pp. 7636–7644, 2023.

[19] F. Gapsari, B. Djarot, Darmadi, H. Juliano, S. Hidayatullah, Suteja, S. M. Rangappa, S. Siengchin, "Modification of palm fiber with chitosan-AESO blend coating," *International Journal of Biological Macromolecules*, vol. 242, no. 4, 2023, Art. no. 125099.

[20] C. Banroongwongdee, S. Gaewkhem and P. Siritrakul, "Kinetics, Equilibrium, and thermodynamics of methyl orange adsorption onto modified rice husk," *KMUTNB International Journal of Applied Science and Technology*, vol. 11, no. 3, pp. 185–197, 2018.

[21] F. Gapsari, L.Djakfar, R. P. Handajani, Y. A. Yusran, S. Hidayatullah, Suteja, S. M. Rangappa, and S. Siengchin, "The application of timoho fiber coating to improve the composite performance," *Results in Engineering*, vol. 15, 2022, Art. no. 100499.

[22] R. Phiri, S. M. Rangappa, S. Siengchin, and D. Marinkovic, "Agro-waste natural fiber sample preparation techniques for bio-composites development: Methodological insights," *Mechanical engineering Series, Facta Universitatis*, vol. 21, no. 4, pp. 631–656, *2023.*

[23] B. A. Ahmed, U. Nadeem, A. S. Hakeem, A. Ul-Hamid, M. Y. Khan, M. Younas, and H. A. Saeed, "Printing parameter optimisation of additive manufactured PLA using taguchi design of experiment," *Polymers*, vol. 15, no. 22, 2023, Art. no. 4370.

[24] P. Aihemaiti, R. Jia, A. Wurikaixi, H. Jiang, and A. Kasimu, "Study on 3D printing process of continuous polyglycolic acid fiber-reinforced polylactic acid degradable composites," *International Journal of Bioprinting*, vol. 9, no. 4, 2023, Art. no. 734.

[25] N. R. Madhan and S. Senthil, "Characterization of tamarind fruit shell power-reinforced virgin and recycled polypropylene-based 3D-printed composites," *Biomass Conversion and Biorefinery*, vol. 14, pp, 13407–13420, 2024.

[26] P. Ghabezi, T. Flanagan, and N. Harrison, "Short basalt fibre reinforced recycled polypropylene filaments for 3D printing," *Materials Letters*, vol. 326, 2022, Art. no. 132942.

[27] V. Chairgulprasert and H.Waehayee, "Removal

of methylene blue dye in water using longkong fruit peels," *KMUTNB International Journal of Applied Science and Technology*, vol. 11, no. 4, pp. 287–295, 2018.

[28] D. L. Vinay, R. Keshavamurty, S. Erannagari, A. Gajakosh, Y. D. Dwivedi, D. Bandhu, N. Tamam, and K. K. Saxena, "Parametric analysis of processing variables for enhanced adhesion in metal-polymer composites fabricated by fused deposition modeling," *Journal of Adhesion Science and Technology*, vol. 38, no. 3, pp. 331–354, 2023.

[29] J. Nomai, B. Suksut, and A. K. Schlarb, "Crystallization behavior of poly(lactic acid)/ titanium dioxide nanocomposites," *KMUTNB International Journal of Applied Science and Technology*, vol. 8, no. 4, pp. 251–258, 2015.

[30] M. Müller, P. Jirků, V. Šleger, R. K. Mishra, M. Hromasová, and J. Novotný, "Effect of infill density in FDM 3D printing on low-cycle stress of bamboo- filled PLA-based material," *Polymers*, vol. 14, no. 22, 2022, Art. no. 4930.